JOURNAL OF CATALYSIS **159,** 31–40 (1996)
ARTICLE NO. 0061

Effect of Silicon Oxide Thickness on the Direct Synthesis of Dimethyldichlorosilane

Sefa Yilmaz, Nicole Floquet,[1] and John L. Falconer

Department of Chemical Engineering, University of Colorado, Boulder, Colorado 80309-0424

Received January 23, 1995; revised October 30, 1995; accepted October 31, 1995

The effect of silicon oxide thickness on the direct synthesis of dimethyldichlorosilane ($(CH_3)_2SiCl_2$, dmd) was studied by reacting Si(100) surfaces with CH_3Cl. Oxide layers of 0.9, 2, 4, and 14 nm average thicknesses were grown on Si(100) and were characterized by ellipsometry and AES. A copper catalyst (82 wt% Cu and 18 wt% Cu_2O) was placed as a powder on the oxide layer and the reaction was carried out at 598 K in 1 atm CH_3Cl. Reacted surfaces were characterized by XRD, SEM, and optical microscopy. The reacted surfaces contained Cu_3Si, Cu, and Si. The surface with the lowest oxide coverage had the best selectivity (78 mol% $(CH_3)_2SiCl_2$ and 22 mol% CH_3SiCl_3). As the oxide thickness increased, the selectivity for $(CH_3)_2SiCl_2$ continuously decreased, the overall reaction rate for methylchlorosilane formation decreased, and the induction time before dmd formation increased. Even after 18 h of reaction, the rate and selectivity were still affected by the initial oxide thickness on the 2-nm oxide surface, but selectivity for dmd on the 4-nm oxide surface was the same as that on the 2-nm oxide surface. The reaction rate on Si(100) with a 14-nm oxide layer was less than 1% of that on the Si(100) with 0.9-nm oxide. On all surfaces, square-based pyramidal pits formed as Si were removed, and the pits were larger, for the same reaction time, for surfaces with thinner oxides. A 4-nm oxide affected the orientation of the Cu_3Si phase, but on 0.9 and 2-nm oxide layers, Cu_3Si was randomly oriented. © 1996 Academic Press, Inc.

INTRODUCTION

Methylchlorosilanes (mcs) are produced industrially in fluidized bed reactors by the Rochow direct synthesis reaction of solid silicon with gaseous methyl chloride (CH_3Cl) (1). Copper catalyzes the selective formation of dimethyldichlorosilane ($(CH_3)_2SiCl_2$, dmd),

$$2CH_3Cl(g) + Si(s) \rightarrow (CH_3)_2SiCl_2(g),$$

which is used as a precursor for the production of linear silicone polymers (2, 3). Without copper, silicon does not react readily with CH_3Cl, and when it does react, dmd is not a significant product (4). High selectivity is desired for the formation of dmd because the other products that form, particularly methyltrichlorosilane (CH_3SiCl_3, mtc), are difficult to separate from dmd. Removal of mtc is necessary because it causes chain branching during the subsequent processing steps, whereas dmd forms the desired linear silicone polymers. Moreover, the other products such as mtc are not as useful and can be made by other reactions.

The Rochow synthesis is sensitive to the purity of silicon, the form of the catalyst, and the presence of promoters. To better understand the surface chemical processes in this solid catalyzed, gas–solid reaction, the surface conditions need to be controlled so that the surfaces can be characterized before and after reaction. Single crystal silicon serves as an ideal surface for this reaction because it is readily available and inexpensive. Moreover, metal/Si and SiO_2/Si interfaces have been studied extensively. Most laboratory studies of the direct synthesis reaction, however, have used conditions that are similar to those in industrial processing: technical grade silicon powders in fluidized beds (1, 5, 6). A few studies have used bulk Cu–Si alloys made from high purity materials (7–9), and one recent study used high purity silicon particles in a packed bed reactor (10).

Hutchings *et al.* (11) used silicon particles to investigate the effect of silicon oxide on the dmd formation rate in a stirred bed reactor. They found no correlation between the surface and bulk oxide content, but for oxide thicknesses from 0.5 to 2.5 nm, they saw a correlation between oxide thickness and reactivity. The rate dropped as the oxide thickness increased. The oxide thickness was calculated from the SiO_2/Si ratio obtained by XPS. They noted that the initial oxide thickness is important in determining reactivity, but it is not the sole factor and thus there was scatter in the correlation. The oxide was not found to be a major factor in selectivity to dmd formation, and impurities present in the Si were more important.

Banholzer *et al.* (12) looked at oxide effects in the direct synthesis by placing single crystal Si wafers into a fluidized bed of Si particles plus catalyst. When the Si wafers were etched with HF to remove the native oxide layer, the entire surface reacted, as measured by SEM. In the absence of HF cleaning, discrete pits were observed. Because of the

[1] On leave from Universite de Bourgogne, Laboratorie de Recherche sur la Reactivite des Solides, B.P. 138, 21004 Dijon Cedex, France.

0021-9517/96 $18.00

presence of the Si particles with high surface area, it was not possible to determine if the selectivity changed since products formed from the single crystal wafers could not be detected. They suggested that their CuCl catalyst deposited at defects in the native SiO_2. Etching with HF increased the defect density so that more Cu deposited and more Si reacted. For a surface coated with a 20-nm oxide, less defects were present and the surface was unreactive.

Suzuki *et al.* (13) likewise observed that a SiO_2 layer slows the rate of the Cu-catalyzed reaction between CH_3OH and Si to form methoxysilanes. When the oxide was removed from Si particles by HF, the reaction rate was much faster. When samples with and without oxide were compared at the same conversion, pits detected by SEM were larger and fewer in number if the oxide layer was present. The oxide layer still had an effect even after 5 h of reaction.

We have shown that semiconductor-grade, single crystal silicon surfaces react with CH_3Cl to form dmd (14). More recently, we reported that high rates and high selectivities to dmd can be obtained with the proper choice of catalyst (15, 16). The same products detected for powders in fluidized beds were observed for Si(100) surfaces. High selectivities were maintained for long reaction times with a 82 wt% Cu/18 wt% Cu_2O powder mixture as a catalyst, which was physically placed on Si(100) surfaces. When other methods of catalyst addition or other compositions of Cu/Cu_2O powders were used, selectivities were lower and methyldichlorosilane (CH_3SHiCl_2) formed a longer reaction times. These previous studies (14, 15) used Si(100) with a 2-nm oxide layer.

For the industrial reaction, the original silicon particles have a native oxide layer of approximately 2 nm. As particles break apart in the fluidized bed reactor, fresh silicon surfaces that are free of oxide are also likely to be exposed. The oxide layer on particles is nonuniform and the oxide thickness is difficult to characterize. Thus, it is of interest to start with surfaces for which the oxide thickness can be measured to determine how the oxide layer affects selectivity. In the current study, we used a 82 wt% Cu/18 wt% Cu_2O catalyst mixture on Si(100) to study the effect of oxide. Preliminary results on the effect of oxide thickness have been reported (16). On flat single crystal surfaces the oxide thickness can be controlled by oxidation conditions and measured by ellipsometry and Auger electron spectroscopy (AES). Thicknesses from 0.9 to 14 nm were used.

Samples were characterized by X-ray diffraction (XRD) and scanning electron microscopy (SEM) after catalyst addition and heat treatment. Reaction with CH_3Cl was carried out at 1 atm and 598 K in a recirculating batch reactor (17). After long reaction times, which were used to verify that selectivities were maintained and that products with long induction times were detected, the solid products of the reaction were characterized by XRD, SEM, and light microscopy.

EXPERIMENTAL METHODS

Sample Preparation

All reactions were carried out on semiconductor-grade (99.9996% purity) Si(100) wafers obtained from Virginia Semiconductor. The silicon wafers had resistivities of 0.1 Ω-cm and were *n*-type, with phosphorus concentrations of approximately 10^{17} atoms/cm^3. Samples were degreased in a 1 : 1 : 1 mixture of methanol, diethylether, and trichloroethane, rinsed in distilled water, and dried in air. To prepare surfaces without an oxide layer, the Si(100) samples were first oxidized in boiling $H_2SO_4 : H_2O_2$ (1 : 1) for 20 min and then etched in 48% HF for 10 min at room temperature to remove the oxide layer. The samples were then rinsed in distilled H_2O, dried in air, and mounted in the sample holder. Samples were heated resistively to 1273 K in UHV and held there four times for 40 s each to remove carbon and oxygen, which were detected by Auger electron spectroscopy. Samples with a native oxide layer were prepared by placing degreased samples in boiling $H_2SO_4 : H_2O_2$ (1 : 1) for 20 min to oxidize any impurities on the surface. A 4-nm oxide layer was prepared by dipping the sample in boiling 70% HNO_3 for 5 mm. A 14-nm oxide layer was grown by thermal oxidation at 1175 K in a dry O_2 stream for 10 min. The oxide thicknesses were estimated by ellipsometry (Gaertner L116C system, 632.8 nm wavelength). The native oxide layer was 2.0 $\pm$ 0.1 nm thick, the oxide layer formed in boiling HNO_3 was 4 $\pm$ 0.2 nm thick, and the thermal oxide layer was 14 $\pm$ 0.7 nm thick.

The samples were mounted in a holder so they could be resistively heated for reaction. Chromel-alumel thermocouple wires were spot-welded to a thin strip of tantalum foil, which was wrapped around the sample edge. Samples were moved into the UHV chamber, which was attached to the reaction chamber, and characterized by AES before copper deposition.

A mixture of Cu (Aldrich, 99.999% pure, 40 μm) and Cu_2O (99.9%, Strem Chemicals Inc., 1.5 to 5 μm) powders was ground with a pestle and mortar, and 15 mg of the mixture were physically placed on the silicon surface. The sample was then resistively heated under UHV and held at 650 K for 1 h.

Reaction Procedure

Reaction kinetics were measured in a combined UHV/atmospheric pressure system. The details of this system have been described previously (17). A bellows transfer mechanism allowed samples to be moved between UHV and the atmospheric pressure reactor without exposure to air. A silicon sample (1 cm^2 surface area) on which the Cu/Cu_2O mixture was deposited was reacted with CH_3Cl at 598 K and atmospheric pressure. A metal bellows pump recirculated the CH_3Cl over the silicon samples, and the conversion of

CH_3Cl was kept below 15% to minimize effects of reaction products. The reaction products were analyzed with a gas chromatograph equipped with a thermal conductivity detector, and product concentrations versus time were used to calculate the reaction rates. The GC column was able to separate the methylchlorosilanes of interest, but the non-silicon-containing products (nonsilanes) were not separated from each other. The nonsilanes are mostly CH_4 (10) and thus CH_4 was used for their calibration. Reaction times were 18 h for the 0.9, 2.0, and 4.0-nm surfaces, and 12 h for the 14-nm oxide surface. Product selectivities were calculated from instantaneous rates that were determined from slopes of concentration versus time plots.

Surface and Bulk Analysis

The surface oxides were characterized by AES before deposition of the catalyst. A PHI cylindrical mirror analyzer was used with a beam energy of 3 keV and a beam current of 30 μA. Shifts in the Si(LVV) peak can be used to determine the Si chemical environment. The Si(LVV) transition at 92 eV is due to elemental Si and the peak at 76 eV is Si bonded to oxygen. The ratio of O (510 eV) to Si (92 eV) peak intensities was used to estimate the oxide thickness of the sample whose oxide was removed in UHV but it was then exposed to air for 3 min.

Reacted samples were removed from the reactor and examined by optical microscopy (Nikon), scanning electron microscopy (Cambridge S250 MK3 and ISI SX 30), and X-ray diffraction to identify surface species. The X-ray (θ, 2θ) powder diffractometer (Scintag, Inc., PAD V) uses Cu$K\alpha$ ($\lambda = 0.154$ nm) radiation and a back-monochrometer to filter Cu$K\beta$ radiation. Solid products were identified by using both JCPDS reference files (18) and literature data (19). The Cu_3Si phase was identified by the *d*-spacings at 0.203, 0.201, 0.143, and 0.117 nm (15). The two major Cu_3Si peaks, Cu_3Si(0 2 9) at $d = 0.201$ nm and Cu_3Si(38 0 0) at $d = 0.203$ nm, were used to determine if the Cu_3Si phase was oriented on the surface.

RESULTS

AES Analysis

Figure 1 shows Auger spectra for Si(100) samples with the four oxide thicknesses used in the reaction studies and a clean Si(100) sample prepared in UHV. Only the region of the spectra that has elemental Si (92 eV) and Si–O (76 eV) is shown. All spectra were recorded before catalyst deposition. No oxide was present on the clean surface since the 76 eV peak is absent in Fig. 1a and no oxygen peak was observed at 510 eV (Table 1). When the clean surface was exposed to air for 3 min, which corresponds to the exposure time required to place the catalyst mixture on the Si surface, the surface oxidized. As a result, the O (510 eV) and Si–O (76 eV) signals increased and the Si (92 eV) signal

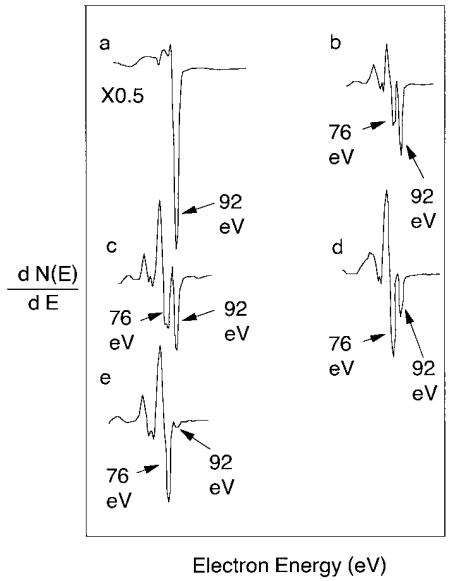

FIG. 1. Silicon Auger spectra for Si(100) surfaces with various oxide layers. The elemental Si (92 eV) and the Si–O (76 eV) transitions are shown: (a) clean Si prepared in UHV; (b) clean Si prepared in UHV and exposed to air for 3 min at room temperature; (c), (d), (e) Si with 2-, 4-, and 14-nm oxide layers, respectively.

decreased. The resulting oxide thickness was estimated by comparing the AES spectra to the Si (92 eV) and O (510 eV) AES intensities of the silicon surfaces whose oxide thicknesses were measured by ellipsometry. As shown in Figs. 1c–1d and Table 1, as the oxide thickness increased, the O (510 eV) Auger peak increased, the Si (92 eV) peak decreased, and the Si–O (76 eV) peak increased.

The relationship between the oxide thickness (t) and the AES intensity ratio is (20–23)

$$\frac{I_O}{I_{Si}} = \frac{I_O^\infty}{I_{Si}^\infty} \cdot \frac{\left[1 - \exp\left(\frac{-t}{\lambda_O \cdot \cos\theta}\right)\right]}{\exp\left(\frac{-t}{\lambda_{Si} \cdot \cos\theta}\right)}, \qquad [1]$$

where I_O represents the O(KLL) intensity at 510 eV and I_{Si} represents the Si(LVV) intensity at 92 eV. This equation was used to estimate an oxide thickness of 0.9 nm from the spectra in Fig. 1b. Chou *et al.* (24) reported 1.3-nm thick oxide layer after air exposure of a bare Si surface. The intensity of the 14-nm oxide layer is I_O^∞ and that of a clean surface is I_{Si}^∞. The λ_O and λ_{Si} values correspond to inelastic mean free paths for oxygen and Si Auger electrons in SiO_2, respectively. These values were estimated as 1.8 and 0.8 nm, respectively, from an expression given by Seah and Dench (25). The angle, θ, was 42° for the cylindrical mirror analyzer used.

If the oxide layers were defect free and uniform, the intensity of 92 eV electrons for the 2-nm oxide (measured by ellipsometry) should be 1.1% of that observed from

TABLE 1

Auger Intensities and Oxide Thicknesses of Si(100)

Oxide thickness measured by ellipsometry (nm)	AES intensity (a.u.)		AES ratio $I_{Si}/I_{Si}^{\infty} \times 100$		Oxide thickness calculated from AES (nm)
	O(510 eV)	Si(92 eV)	Calculated	Measured	
0	0	250	—	—	—
0.9	89	46	—	18	0.9
2	170	53	1.1	21	1.1
4	190	27	0.01	10	1.5
14	220	3	10^{-12}	1.2	2.8

the clean surface, as calculated from the relationship (20, 21, 26)

$$\frac{I_{Si}}{I_{Si}^{\infty}} = \exp\left(\frac{-t}{\lambda_{Si} \cdot \cos\theta}\right). \quad [2]$$

Instead, the measured intensity of Si was 21% of that on the clean surface (Table 1). On the 4-nm oxide surface, the measured intensity ratio from AES was more than 1000 times that calculated from Eq. (2). The difference in the Si signal attenuation may be attributed to either defects and pinholes in the oxide layer or over-estimation of the oxide thickness by ellipsometry. As shown in Table 1, the oxide thicknesses measured by ellipsometry are significantly different from those estimated from the Auger intensities. For the 14-nm oxide, Auger clearly underestimates the oxide thickness since the ellipsometry measurements of thicker oxides are more reliable (26–28). The silicon intensity ratio ($I_{Si}/I_{Si}^{\infty} \times 100$) for the 0.9-nm oxide surface (18%) is approximately equal to that of 2-nm oxide surface (21%), although O (510 eV) and Si–O (76 eV) Auger signals were much smaller on the 0.9-nm oxide than on the 2-nm oxide surface.

Kinetic Measurements

As shown in Figs. 2–4. CH_3Cl reacted to form methylchlorosilanes on Si(100) surfaces that had oxide layers of 0.9, 2.0, and 4.0 nm. No products were detected, however, from the 14-nm oxide surface during 600 min of reaction. Several similarities were observed for the surfaces with oxide layers of 0.9, 2.0, and 4.0 nm.

- Methylchlorosilane (mtc) was the first product to form.
- Dimethyldichlorosilane (dmd) had significantly longer induction times than mtc, and dmd was the dominant product at longer time.
- Rates of dmd and mtc formation decreased at longer times, but selectivity to dmd did not change.
- Trimethylchlorosilane (tmc) was only observed after long times, or not at all, and its concentration was low.

The nonsilane rates were similar on the 0.9 and the 4.0 nm oxide surfaces and were 2/3 of the nonsilane rate on the 2-nm oxide surface. On the 14-nm oxide layer, only nonsilanes formed and at 1/3 the rate observed on the 2-nm oxide surface.

One interesting aspect of the kinetic data in Figs. 2–4 is that even after long reaction times and many layers of silicon had reacted (10^4 layers on the 2-nm oxide and 3×10^3 layers on 4-nm oxide), the rates and selectivities were different for the 0.9 and 2-nm oxide surfaces. The selectivities on the 2- and 4-nm oxides were similar. Several trends were observed as the oxide thickness increased:

- Induction times for dmd and tmc increased (Table 2). The induction times were estimated by extrapolating concentrations to zero. The induction time for mtc did not change much with oxide thickness.
- The rate of formation of each methylchlorosilane decreased.
- Selectivity for dmd formation decreased.

Figure 5 shows the trends in dmd selectivity (based on rates) with oxide thickness at four reaction times. Because of the longer induction time for dmd than mtc, the dmd selectivity increased during the induction period, and hence selectiv-

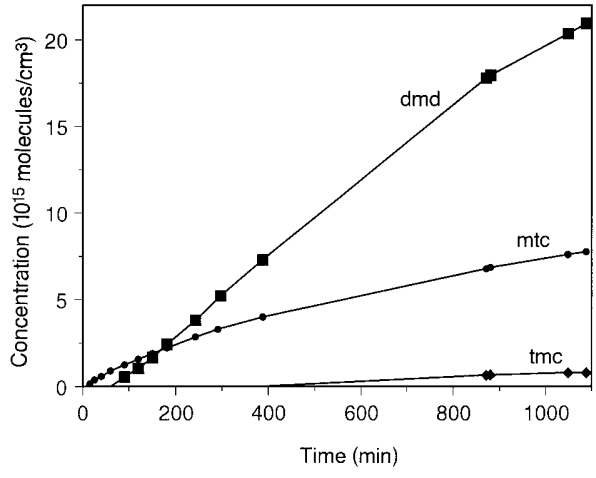

FIG. 2. Methylchlorosilane concentration versus time plots for reaction of methyl chloride with Si that has a 0.9-nm oxide surface (1 cm^2 surface area).

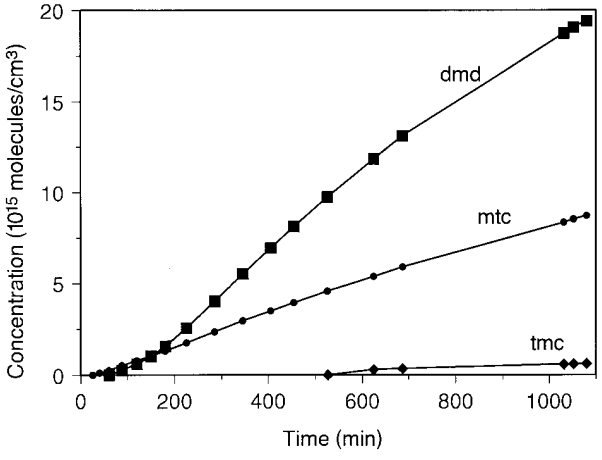

FIG. 3. Methylchlorosilane concentration versus time plots for reaction of methyl chloride with Si that has a 2-nm oxide surface (1.24 cm^2 surface area).

ities at 400 min were higher than those at 200 min. The highest selectivity for dmd formation was 78 mol% on the Si(100) with 0.9-nm oxide layer. This surface also had the highest rate, as shown in Fig. 6.

Experiments were repeated on the 0.9- and 2-nm oxide surfaces with fresh samples and fresh catalyst mixtures. The dmd selectivities as a function of time are almost identical and average selectivities are presented in Fig. 5. Rates differed because of the difficulty in spreading the catalyst uniformly on the surface, and optical microscopy showed that the surface with higher methylchlorosilane formation rate had a higher catalyst coverage. When the rates were normalized per cm^2 of Si surface area that was covered with the catalyst (as measured with the optical microscope), similar rates were obtained. Hence, rates presented in Fig. 6 and

TABLE 2

Induction Times for Methylchlorosilane Products

Oxide thickness (nm)	Induction time (min)		
	$(CH_3)_2SiCl_2$	CH_3SiCl_3	$(CH_3)_3SiCl$
0.9	75	15	460
2	75	25	630
4	120	25	>1100
14	>600	>600	>600

Table 3 were normalized by the Si area covered with catalysts. Selectivities were not affected by the change in the catalyst coverage. The XRD patterns for the repeated experiments on 0.9- and 2-nm oxide surfaces also had good reproducibility.

Analysis of Reacted Samples

An SEM image of the 0.9-nm oxide surface after reaction showed a rough surface that consisted of a large number of interconnected pits (Fig. 7a). No unreacted areas were present and the Si substrate had a sponge-like appearance after reaction. Analysis by XRD detected Cu_3Si and Cu, but no Cu_2O. Copper spheres (Fig. 7b) were identified by their gold color under optical microscopy (15, 29), and their mean crystallite size was estimated as 0.1 μm from the diffraction peak half-width (30). The Cu_3Si XRD peaks were smaller than those from 2- and 4-nm oxide surfaces after reaction, and the ratio of Cu_3Si(0 2 9) to Cu_3Si(38 0 0) peaks was 0.77 $\pm$ 0.14. This ratio was close to the value of 0.6 obtained for a randomly-oriented Cu_3Si powder (15).

Both discrete square pits and interconnected pits were detected by SEM on the 2-nm oxide surface after reaction

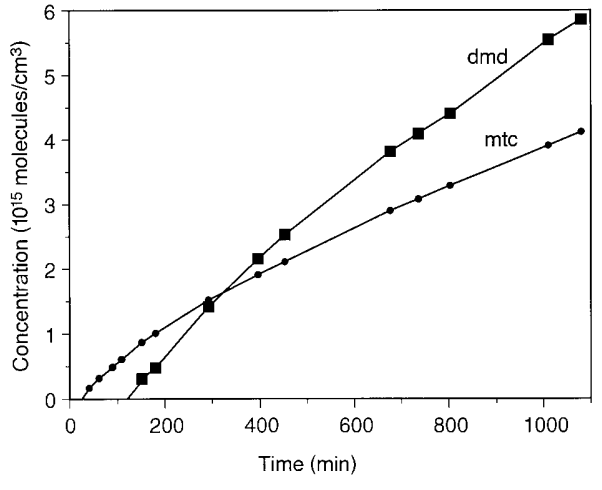

FIG. 4. Methylchlorosilane concentration versus time plots for reaction of methyl chloride with Si that has a 4-nm oxide surface (0.76 cm^2 surface area).

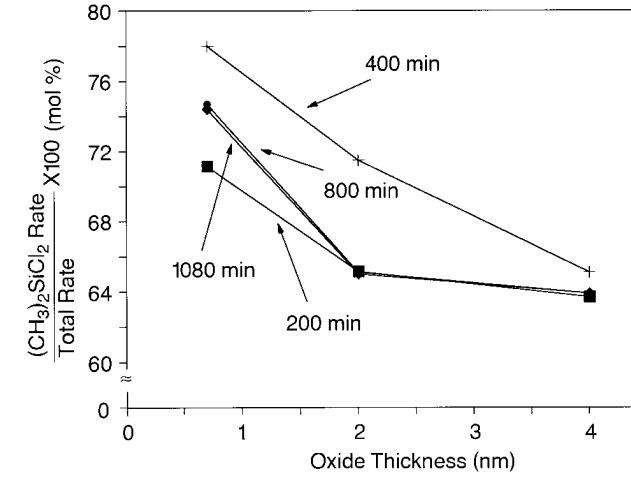

FIG. 5. $(CH_3)_2SiCl_2$ (dmd) mol% based on rates at 200, 400, 800, and 1080 min versus the oxide thickness.

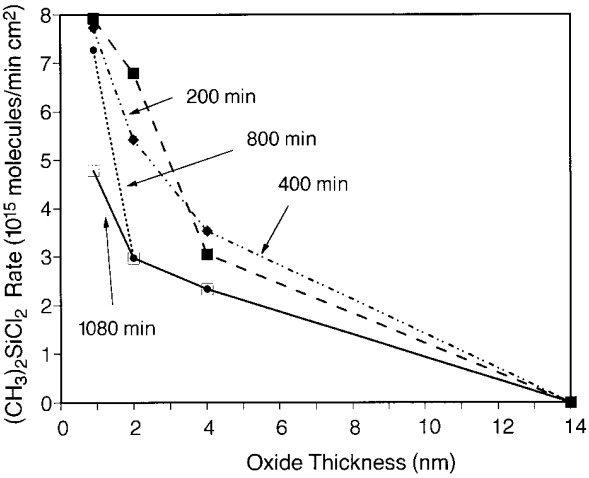

FIG. 6. $(CH_3)_2SiCl_2$ formation rate at 200, 400, 800, and 1080 min versus the oxide thickness.

(Fig. 7c). The discrete pits looked like inverted pyramids and were 4–10 μm wide and partially full of Cu_3Si, as determined by optical microscopy and XRD (15). Both Cu and Cu_3Si phases were detected by XRD and the total intensity of Cu_3Si peaks was twice that observed on the 0.9-nm oxide surface. The $Cu_3Si(0\ 2\ 9)/Cu_3Si(38\ 0\ 0)$ intensity ratio was 0.41 ± 0.16, which indicates a Cu_3Si orientation close to random.

Similarly, both discrete and interconnected pits were detected by SEM on the 4-nm oxide surface (Fig. 7d). The pits were smaller (1–5 μm) than for the 2-nm oxide surface and the density of the pits also was lower. An XRD analysis detected Cu, Cu_3Si, and small amounts of CuO. The total intensity of Cu_3Si peaks was greater than that on 2-nm oxide surface. The intensity ratio $Cu_3Si(0\ 2\ 9)/Cu_3Si(38\ 0\ 0)$ was 1.4, which indicates that Cu_3Si was partially oriented on the surface.

Though no methylchlorosilanes were detected by GC for the Si(100) surface with the 14-nm oxide, discrete pits (1–3 μm) were detected by SEM (Fig. 7e). That is, the surface appeared to react, but only 5% of the exposed surface area was covered by pits as opposed to 80% for 2-nm oxide surface, indicating that the rate of reaction on the 14-nm oxide surface was much lower. The pit formation may also be due at least partially to the reaction of Cu_3Si with CuCl that formed during the reaction with CH_3Cl, as suggested by Viale *et al.* (31),

$$Cu_3Si + 4\,CuCl \rightarrow SiCl_4 + 7\,Cu,$$

although no $SiCl_4$ was detected. X-ray diffraction detected small amounts of Cu_3Si, Cu, and CuO on the surface, and the catalyst particles were loose and most of them dropped off the surface during the XRD analysis. The Cu_3Si phase was tightly held in the pits. On the thinner oxides the catalyst particles were held on the surface after reaction and tilting did not cause any loss in particles.

TABLE 3

Total Reaction Rate (10^{15} molecules/min cm^2) of Methylchlorosilane Products

	Oxide thickness (nm)		
Time (min)	0.9	2	4
200	10.8 ± 2.6	8.3 ± 0.2	5.5
400	10.2 ± 1.9	9.5 ± 0.9	4.7
800	7.7 ± 3.1	5.6 ± 1.2	3.7
1080	4.8 ± 2.1	5.6 ± 1.2	3.7

DISCUSSION

Nonuniform Oxide

The Auger Si(LVV) spectra has two major peaks, at 76 and 92 eV, that correspond to SiO_2 and elemental Si, respectively (32). The elemental Si substrate signal decreased as it was attenuated by the growing oxide, and the SiO_2 signal increased with the oxide thickness (Fig. 1). For a uniform 2-nm oxide layer, the signal amplitude of the 92 eV peak should be 1.1% of that observed on a clean (oxide free) surface, but the measured amplitude was 21% of that for the clean surface (Table 2). This higher intensity is probably due in part to defects and pinholes, which are known to occur in thin oxide layers (23, 34, 35). In addition, thicknesses measured by ellipsometry tend to be higher than these measured by Auger (26–28). Chang and Boulin (27) reported that ellipsometry-measured thicknesses were as much as twice those from Auger. They proposed that the difference is due largely to the finite extent of the oxide/Si interface, and the measurement of the interface by using different physical parameters.

Oxide films that are 1–20 nm thick contain defects such as pinholes, voids, or pores formed during the film growth. Direct evidence of pores or voids has been obtained by high resolution transmission electron microscopy (33). These pores or voids may be up to 1 nm in diameter and 10 nm apart in a 9-nm thick, dry thermal oxide layer. As the oxide layer gets thicker, the surface density of these defects gets smaller (23, 34, 35).

The contact between the silicon substrate and catalyst probably takes place through pinholes or defects present in the oxide layer since Cu does not react with SiO_2 (12, 36). When Cu contacts Si underneath the oxide layer, copper-silicides form (29). Silicide formation is inhibited by a thicker oxide. For example, no silicide formation was observed upon evaporation of Cu on a 200-nm thick oxide surface even after annealing for 3 h at 1073 K (36). Apparently, the defect concentration was low. Hattori *et al.* (23, 35) showed that the surface density of the defects de-

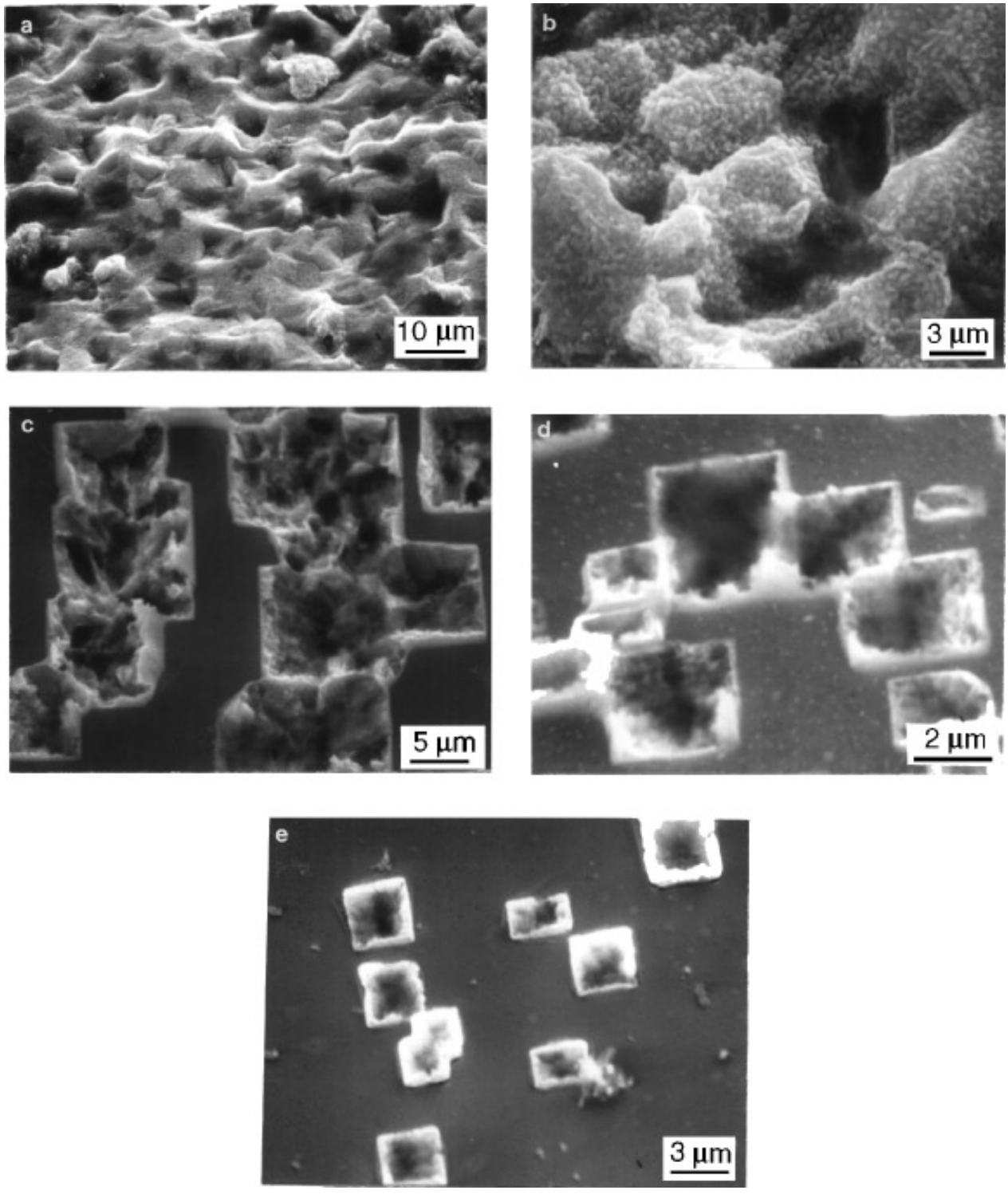

FIG. 7. SEM images after reaction with CH_3Cl: (a) and (b) 0.9-nm oxide surface, (c) 2-nm oxide surface, (d) 4-nm oxide surface, and (e) 14-nm oxide surface.

creased exponentially as the oxide thickness increased. An oxide thickness of 20 nm was sufficient to completely block the reaction between silicon and CH_3Cl (12).

Our SEM pictures indicate that the density of the interconnected and discrete pits decreased and their sizes also decreased as the oxide thickness increased. The 14-nm oxide surface had only discrete pits and no interconnected pits. The decrease in both the size and density of defects as oxide thickness increased means that less silicon area was available for the catalyst mixture to contact (37). Souha *et al.* (37) showed that the number of Cu_3Si patches that form from the reaction of Si and CuCl decreased as the oxide thickness increased. This indicated that the SiO_2 layer does not react with CuCl, and this layer acts as a barrier for the reaction of Si and Cu (37). The decrease in the contact area between Si and Cu results in a decrease in rate of formation of both dmd and mtc as oxide thickness increases (Fig. 6).

Even if not many pinholes or defects are present in the original oxide layer, the catalyst may help form additional defects. When metals are deposited in the SiO_2 surface, defects in the oxide can be induced upon annealing between 673 and 1273 K (38, 39). Liehr *et al.* (38) reported that the deposition of a monolayer of a transition metal (Cu, Au, Ag, W, Ni, Pt) on a 20-nm, dry thermal oxide induced the formation of distinct voids that were significantly larger than those on the oxide surface upon annealing without the metal. The voids were detected by scanning Auger microscopy. These metals do not react with SiO_2 (36), but they diffuse to the SiO_2–Si interface and donate their *d*-band electrons to a Si–O bond to form volatile SiO species near the interface at 673 K (38). This causes a defect to form and defects grow linearly with time (40).

Activity and Selectivity

Souha *et al.* (37) reported that different copper silicides formed (Cu_3Si, Cu_5Si, $Cu_{15}Si_4$) after deposition of CuCl on different thicknesses of silicon oxide. In the current study, only Cu_3Si was detected, and the orientation of the Cu_3Si phase was different for the surfaces with different oxide thicknesses.

As shown previously (15), Si(100) with an oriented Cu_3Si phase tends to give poorer selectivities for dmd than Si(100) with a random Cu_3Si phase. The Cu_3Si phase was randomly oriented on 0.9 and 2-nm oxide surfaces since the $Cu_3Si(0\ 2\ 9)/Cu_3Si(38\ 0\ 0)$ ratio was close to the value of 0.6 obtained for a Cu_3Si powder. This ratio was 1.4 for the 4-nm oxide surface and indicated that the Cu_3Si phase was partially oriented on that surface. Though the orientation of Cu_3Si on the 4-nm oxide surface is quite different from that on 2-nm oxide, selectivity for dmd on the 4-nm oxide is only slightly lower than that on the 2-nm oxide. Thus, the decrease in selectivity as the oxide thickness increases is not mainly a result of preferentially-oriented Cu_3Si.

The decrease in the rate of formation of methylchlorosilanes with oxide thickness can be attributed to the decrease in the silicone surface area available for the catalyst to contact. The number of Cu_3Si nuclei formed when CuCl vapor reacted with a Si(100) surface decreased a factor of 4 when the oxide thickness increased from 0.6- to 2-nm (34). Viale *et al.* (34) attributed this decrease to the decrease in the number of defects as the oxide thickness increased. Despite the decrease in the number of pits in our study due to the increase in the oxide layer, the total XRD peak intensities of the Cu_3Si phase and thus the amount of Cu_3Si increased. Thus, there was no correlation between the amount of Cu_3Si detectable by XRD after reaction and the rate of methylchlorosilane formation.

The induction time for methylchlorosilane formation increased as the oxide thickness increased, except that induction times for 0.9- and 2-nm oxide surfaces were similar. The induction time may be related to the defect density. The smallest induction times for dmd, mtc, and tmc were observed on the 0.9- and 2-nm oxide surfaces, and the largest defect density is expected on these surfaces.

Comparison to Literature

We previously studied (14) the effect of oxide thickness on the direct synthesis reaction by decomposing copper (II) formate deposited from solution. The decomposition products were a mixture of Cu and Cu_2O particles on a Cu film and their composition was sensitive to the concentration of the solution. The oxide layer appeared to enhance the selectivity for dmd, but mdc was a major product on all surfaces at longer times, and thus these surfaces were poorer models of the direct reaction surface than those used in the current study.

Banholzer *et al.* (12), who used single crystal Si wafers in fluidized bed reactors that contained Si particles and catalyst, found that as the oxide was removed by HF, the reaction rate increased. They determined that the rate increased from SEM analysis of the Si wafers. Our results, with direct measurement of the products formed from the Si single crystal surfaces, show that both the rate and the selectivity increase as the oxide thickness decreases. Similarly, Banholzer *et al.* reported that a 20-nm oxide layer was sufficient to passivate the surface, and we see that a 14-nm oxide dramatically decreases the rate such that no gas phase products were detectable in our system. Our results are also in agreement with those made by Hutchings *et al.* (11) for Si particles in a stirred bed reactor. They observed that as the oxide thickness increased the rate decreased. The oxide thickness was measured by XPS. They could not see any correlation between oxide thickness and selectivity, but the impurities in their Si affected selectivity.

De Cooker *et al.* (41) studied the effect of O_2 in the CH_3Cl feed on the direct synthesis reaction. They used a mixture of Cu and Si powders in a fluidized bed reactor and found

that the introduction of 1000 ppm O_2 in CH_3Cl slightly reduced the selectivity, and 5000 ppm O_2 reduced the selectivity for dmd by 11 mol%. They observed that introduction of 1–1000 ppm O_2 reduced the rate by 35%, but 1000–5000 ppm O_2 reduced the rate only by 11%. They attributed the decrease in the reaction rate to high coverages of adsorbed oxygen on the contact mixture and formation of H_2O due to the presence of H_2 formed from the decomposition of CH_3Cl. Silicon dioxide formation on Si and Cu_3Si can passivate the surface and decrease the rate of reaction. Rong (42) studied the effect of O_2 impurities in the CH_3Cl feed for a fluidized bed reactor and found that the reproducibility of their kinetic data was sensitive to the concentration of O_2 in CH_3Cl. Rong also showed that the reactivity of the contact mass doubled and the selectivity for dmd increased by 50% after removing O_2.

The addition of O_2 in the reaction of alloys of Cu–Si and CH_3Cl showed similar effects on the direct synthesis reaction. Lobusevich *et al.* (43) showed that addition of 7400 ppm O_2 to CH_3Cl decreased reactivity by 40% and selectivity to dmd by 23 wt%. They also reported that oxidation of Cu–Si alloys in air for 1 year decreased the rate and selectivity for dmd (44). They detected SiO_2 and CuO by XRD on air-exposed surfaces before reaction. Agarwala and Falconer (9) studied the effect of oxidation of a Cu_3Si–1.2% Zn alloy on the direct synthesis reaction in a batch reactor. The rate of dmd formation decreased linearly as the surface oxygen concentration increased from 3 to 35 at.%, but the selectivity for dmd was not affected by oxygen. They (9) observed that the CH_3Cl decomposition rate to form nonsilanes increased in the presence of surface oxygen. Furthermore, they showed that the induction times for dmd, mtc, and tmc increased as the surface oxygen concentration increased.

CONCLUSIONS

Both the selectivity and the rate of the direct synthesis reaction to form dimethyldichlorosilane decrease as the silicon oxide thickness increases. The change in orientation of the CH_3Si phase is not the main reason for the selectivity decrease. The induction times before products are detected increase with oxide thickness because the reaction between the catalyst and silicon is slower. Reaction probably starts at pinholes or defects present in the oxide. A 4.0-nm oxide decreases the reaction rate by 50% and the rate on a 14-nm oxide is less than 1% of that on a 0.9-nm oxide. The pit size and density decrease as the oxide thickness increases.

ACKNOWLEDGMENTS

We gratefully acknowledge financial support by Elkem Metals Company and the National Science Foundation, Grant CTS-9317580.

REFERENCES

1. Voorhoeve, R. J. H., "Organochlorosilanes: Precursors to Silicones." Elsevier, Amsterdam, 1967.
2. Rochow, E. G., "An Introduction to the Chemistry of the Silicones." Wiley, New York, 1951.
3. McGregor, R. R., "Silicones and Their Uses." McGraw-Hill, New York, 1954.
4. Frank, T. C., and Falconer, J. L., *Langmuir* **1**, 104 (1985).
5. Ward, W. J., Ritzer, A., Carroll, K. M., and Flock, J. W., *J. Catal.* **100**, 240 (1986).
6. Banholzer, W. F., and Burrell, M. C., *J. Catal.* **114**, 259 (1988).
7. Frank, T. C., Kester, K. B., and Falconer, J. I., *J. Catal.* **91**, 44 (1985).
8. Magrini, K. A., Falconer, J. L., and Koel, B. E., *in* "Catalyzed Direct Reactions of Silicon" (K. M. Lewis and D. G. Rethwisch, Eds.), p. 249. Elsevier, Amsterdam, 1993.
9. Agarwala, J. P., and Falconer, J. L., *Int. J. Chem. Kinet.* **19**, 519 (1987).
10. Gaspar-Galvin, J. P., Sevenich, D. M., Friedrich, H. B., and Rethwisch, D. G., *J. Catal.* **128**, 468 (1991).
11. Hutchings, G. J., Joyner, R. W., Siddiqui, M. R. H., and Rong, H. M., *in* "Silicon for the Chemical Industry," (H. A. Øye and H. Rong, Eds.), p. 85. Geiranger, Norway, 1992.
12. Banholzer, W. F., Lewis, N., and Ward, W., *J. Catal.* **101**, 405. (1986).
13. Suzuki, E., Okamoto, M., and Ono, Y., *Solid State-Ionics* **47**, 97 (1991).
14. Falconer, J. L., and Yilmaz, S., "Silicon for the Chemical Industry" (H. A. Øye and H. Rong, Eds.), p. 99. Geiranger, Norway, 1992.
15. Floquet, N., Yilmaz, S., and Falconer, J. L., *J. Catal.* **148**, 348 (1994).
16. Yilmaz, S., Floquet, N., and Falconer, J. L., *in* "Silicon for the Chemical Industry II" (H. A. Øye and H. M. Rong, L. Nygaard, G. Schüssler, and J. Kr. Tuset, Eds.), p. 137. Geiranger, Norway Tapir Forlag, Trondheim, Norway, 1994.
17. Frank, T. C., Kester, K. B., and Falconer, J. L., *J. Catal.* **95**, 396 (1985).
18. Joint Committee on Powder Diffraction Standards (JCPDS), Standard Powder Diffraction File, International Center for Diffraction Data, Swarthmore, PA.
19. Solberg, J. K., *Acta. Crystallogr. Sect. A* **34**, 684 (1978).
20. Sobolewski, M., and Helms, C. R., *J. Vac. Sci. Technol. A* **3**, 1300 (1985).
21. Brudle, C. R., *J. Vac. Sci. Technol.* **11**, 212 (1974).
22. Ishizaka, A., Iwata, S., and Kamigaki, Y., *Surf. Sci.* **84**, 355 (1979).
23. Hattori, T., Utsugi, Y., and Yamuchi, H., *Thin Solid Films* **97**, 231 (1982).
24. Chou, N. J., van der Meulen, Y. J., Hammer, R., and Cahill, J., *Appl. Phys. Lett.* **24**, 200 (1974).
25. Seah, M. P., and Dench, W. A., *Surf. Interface Anal.* **1**, 2 (1979).
26. Wildman, H. S., Bartholomew, R. F., Pliskin, W. A., and Revitz, M., *J. Vac. Sci. Technol.* **18**, 955 (1981).
27. Chang, C. C., and Boulin, D. M., *Surf. Sci.* **69**, 385 (1977).
28. Raider, S. I., and Flitsch, R., *IBM J. Res. Develop.* **22**, 294 (1978).
29. Weber, G., Gillot, B., and Barret, P., *Phys. Status Solidi* **75**, 567 (1983).
30. Eberhart, J. P., "Structural and Chemical Analysis of Materials." p. 203. 1991.
31. Viale, D., Weber, G., and Gillot, B., *Oxid. Met.* **35**, 415 (1991).
32. Davis, L. E., MacDonald, N. C., Palmberg, P. W., Riach, G. E., and Weber, R. E., "Handbook of Auger Electron Spectroscopy, 2nd ed." Physical Electronics, Eden Prairie, MN, 1976.
33. Gibson, J. M., and Dong, D. W., *J. Electrochem. Soc.* **127**, 2722 (1980).
34. Viale, D., Weber, G., and Gillot, B., *J. Cryst. Growth* **102**, 269 (1990).
35. Hattori, T., *in* "Proceedings, 7th International Vacuum Congress and

3rd International Conference on Solid Surfaces." (R. Dobrozemsky, F. Rudenauer, F. P. Viehbock, and A. Breth, Eds.), p. 2157. Vienna, Berger, 1977.
36. Pretorius, R., Harris, J. M., and Nicolet, M. A., *Solid State Electron.* **21**, 667 (1978).
37. Souha, H., Viale, D., Weber, G., and Gillot, B., *J. Mater. Sci.* **24**, 1767 (1989).
38. Liehr, M., Dallaporta, H., and Lewis, J. E., *Appl. Phys. Lett.* **53**, 589 (1988).
39. Goodnick, S. M., Fathipour, M., Ellsworth, D. L., and Wilmsen, C. W., *J. Vac. Sci. Technol.* **18**, 949 (1981).
40. Liehr, M., Lewis, J. E., and Rubloff, G. W., *J. Vac. Sci. Technol.* **5**, 1559 (1987).
41. De Cooker, M. G. R. T., Van Den Hof, R. P. A., and Van Den Berg, P. J., *J. Organom et. Chem.* **84**, 305 (1975).
42. Rong, H. M., Silicon for the Direct Process to Methylchlorosilanes, Ph.D. Thesis, Institutt for Uorganisk Kjemi, Universitetet I Trondheim, Trondheim, 1992.
43. Lobusevich, N. P., Trofimova, I. V., Andrianov, K. A., and Golubtsov, S. A., *J. Appl. Chem. USSR* **37**, 1150 (1964).
44. Lobusevich, N. P., Golubtsov, S. A., Malysheva, L. A., Lainer, L. I., and Trofimova, I. V., *Zh. Prikl. Khim.* **31**, 635 (1968).